

State of the Art of Two-Terminal Devices as Millimeter- and Submillimeter-Wave Sources

Heribert Eisele and George I. Haddad

Solid-State Electronics Laboratory
Department of Electrical Engineering & Computer Science
The University of Michigan
Ann Arbor, Michigan 48109-2122

ABSTRACT

Devices from three major groups of two-terminal devices, *i.e.*, transit-time diodes, transferred-electron devices, and quantum-well devices, have been employed successfully to generate RF power at frequencies above 200 GHz. At frequencies up to 300 GHz, Si IMPATT diodes yielded the highest RF power levels from any fundamental solid-state source, *e.g.*, 50 mW at 245 GHz. However, the RF power of more than 1 mW from InP Gunn devices around 315 GHz is the highest from any such fundamental source above 300 GHz. GaAs TUNNETT diodes operating as efficient self-oscillating frequency multipliers generated RF power levels of more than 10 mW at 202 GHz. GaAs IMPATT diodes, *e.g.*, yielded 2 mW at 232 GHz. The highest oscillation frequency of 714 GHz was reported from an InAs/AlSb RTD with an RF output power of 0.3 μ W, whereas GaAs/AlAs superlattice electronic devices yielded 0.2 μ W at 224 GHz. This paper reviews the power generation capabilities and basic properties of these two-terminal devices as fundamental RF sources. It compares them directly at the RF power level, but also in terms of RF power per unit area as a figure of merit.

1. INTRODUCTION

Systems for rapidly emerging applications at submillimeter-wave frequencies such as upper atmospheric imagery, remote sensing, array receivers in radio astronomy, high-resolution near-object analysis, and ultra wide bandwidth intersatellite communications require reliable and compact RF sources with low dc power consumption as one of their key components. RF power generation at high millimeter-wave frequencies was already demonstrated with various types of solid-state devices [1] thus making them good candidates for sources at submillimeter-wave frequencies. The practical application of “classical,” but also more recent principles in device physics [2]–[4] resulted in major advances in device performance, which have also been enabled by epitaxial materials of superior properties or quality as well as much improved processing technologies. Amplifiers with three-terminal devices reach higher and higher frequencies [5]–[9], and improvements in their RF output power [10] as well as their increasing use in systems applications are being reported up to millimeter-wave frequencies. Nonetheless, there have been a few practical demonstrations of fundamental oscillators with three-terminal devices above 100 GHz, and, in addition, only low RF power levels of much less than 1 mW were

reported [11], [12]. This paper gives an overview of the basic properties of different two-terminal devices for continuous-wave (CW) RF power generation at submillimeter-wave frequencies and mainly focuses on devices that in the laboratory already yielded RF power at frequencies above 200 GHz.

2. RTDS AND OTHER QUANTUM-WELL DEVICES

Resonant tunneling through discrete energy levels of a so-called quantum well was first demonstrated in 1974 [4]. However, only after major advances in growth techniques, such as molecular beam epitaxy (MBE) and metalorganic chemical vapor deposition (MOCVD), in the 1980s were device structures suitable for oscillators grown and evaluated. As can be seen from Fig. 1, the highest oscillation frequency of any fundamental solid-state RF source were reported from InAs/AlSb resonant tunneling diodes (RTDs) [13], [14]. The dc-to-RF conversion efficiencies, however, are below 1% at millimeter-wave frequencies and the RF power levels of, *e.g.*, 3 μ W at 360 GHz and 0.3 μ W at 712 GHz [14] are low, which severely limits the use of RTDs in systems applications.

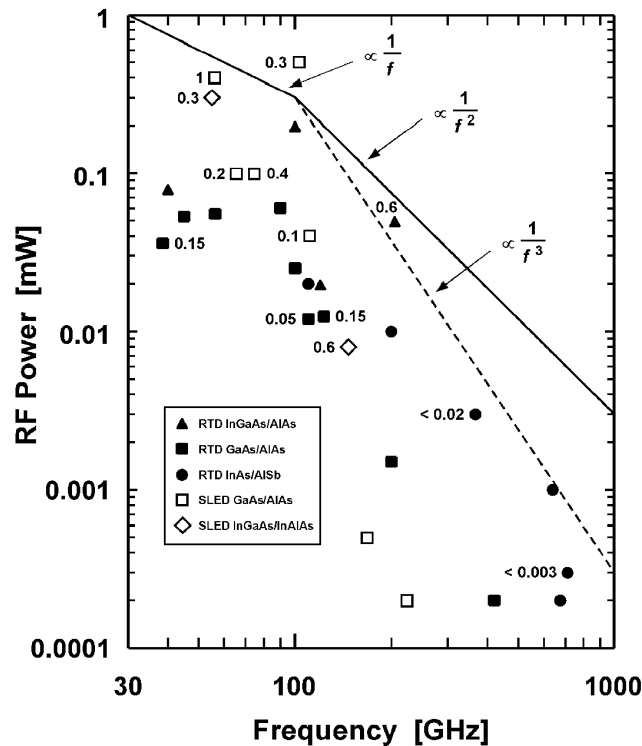


Fig. 1. Published state-of-the art results from RTDs and SLEDs in the 30–1000 GHz frequency range. Numbers next to the symbols denote dc-to-RF conversion efficiencies in percent, where applicable.

More recently, superlattice electronic devices (SLEDs) were demonstrated as millimeter-wave oscillators [15]–[18], and the results are included in Fig. 1. The devices were typically not mounted in a resonant cavity, but they were in quasi-planar structures and were contacted with different ground-signal or ground-signal-ground (GSG) probes for *V*-band (50–75 GHz) or *W*-band (75–110 GHz) [16]–[17]. Exceptions are the quasi-planar circuits in a WR-15/WR-6 waveguide combination [15] and in a WR-6 waveguide as shown in Fig. 2 [18]. As an example, Fig. 2 also illustrates the setup with a GSG probe for *W*-band [17]. RF power levels (and corresponding dc-to-RF conversion efficiencies) of 0.4 mW (1%) were reported at the fundamental frequency of 56 GHz and 40 μ W (0.1%), at the second-harmonic frequency of 112 GHz from the quasi-planar circuit configuration in a waveguide [15]. With the GSG probe and a spectrum analyzer, an RF power of 0.5 mW (0.3%) was determined at 103 GHz [17]. The length of the active region ranges approximately from 0.44 μ m to 0.64 μ m in these GaAs/AlAs SLEDs. Therefore, the higher oscillation frequency of 103 GHz is attributed to much narrower barriers of the quantum wells, which are only two monolayers of AlAs thick and cause a larger miniband width of 120 meV [17]. At a similar length of the active region, an InGaAs/InAlAs SLED generated 80 μ W (0.6%) at the higher oscillation frequency of 147 GHz [18]. Recorded spectra of these SLEDs in free-running oscillators, however, are not as clean as, *e.g.*, those of Gunn devices in free-running oscillators, but are quite narrow-band for a nonresonant circuit or for low quality factors Q .

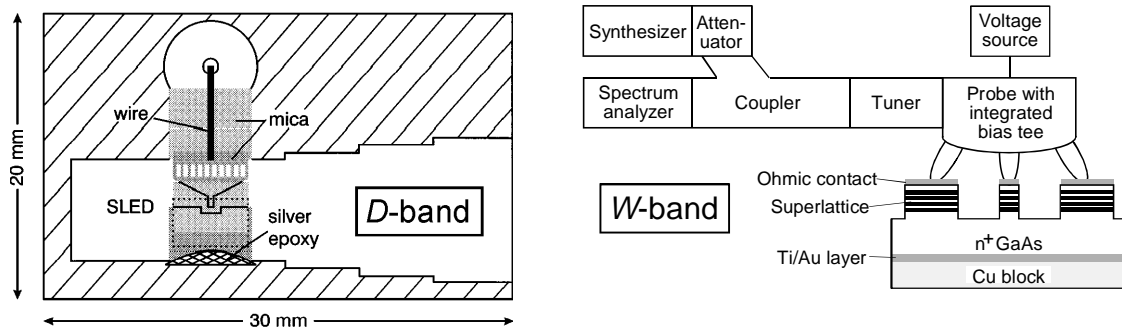


Fig. 2. Experimental setup for evaluation of SLEDs at *W*-band and *D*-band frequencies, respectively. After E. Schomburg *et al.* [17], [18].

Up to *D*-band (110–170 GHz) frequencies, RF power levels from SLEDs are higher than those from RTDs of the same material system, whereas dc-to-RF conversion efficiencies are comparable. They are still much lower than the RF power levels from impact avalanche transit-time (IMPATT) and tunnel injection transit-time (TUNNETT) diodes as well as Gunn devices at the same frequencies. These RF power levels P_{RF} were measured with two-terminal devices of quite different device areas A . Therefore, the RF power density $\Phi_{\text{RF}} (= P_{\text{RF}}/A)$ provides a better comparison of the power generating capabilities of various two-terminal devices and should be considered analogous to the performance

comparisons quoted as RF power per gate length for three-terminal devices, such as field-effect transistors (FETs) or high electron mobility transistors (HEMTs). Fig. 3 shows Φ_{RF} as derived from published state-of-the-art results and device areas in the 30–1000 GHz frequency range for device types that, so far, have yielded measurable RF power levels above 200 GHz. As a result of high bias current densities and high dc-to-RF conversion efficiencies, Φ_{RF} is by far the highest in Si and GaAs IMPATT diodes and exceeds that of RTDs, but also SLEDs, up to *D*-band (110–170 GHz) frequencies by typically more than two orders of magnitude. In addition, Φ_{RF} of GaAs TUNNETT diodes and Gunn devices exceeds that of RTDs and SLEDs up to the highest oscillation frequencies as well. Φ_{RF} of SLEDs from the GaAs/AlAs material system is only higher than that of RTDs from the same material system, but, quite importantly, SLEDs are not associated with the same severe restrictions [1], [19] that bias instabilities impose on the device areas and, consequently, the RF power generation capabilities of RTDs. Therefore, higher RF power levels can be expected from SLEDs with larger areas in appropriate millimeter-wave circuits that match the resulting lower device impedance levels to the RF load. Furthermore, the experimental result at 103 GHz [17] indicates the potential of reaching higher oscillation frequencies with GaAs/AlAs SLEDs than with GaAs Gunn devices.

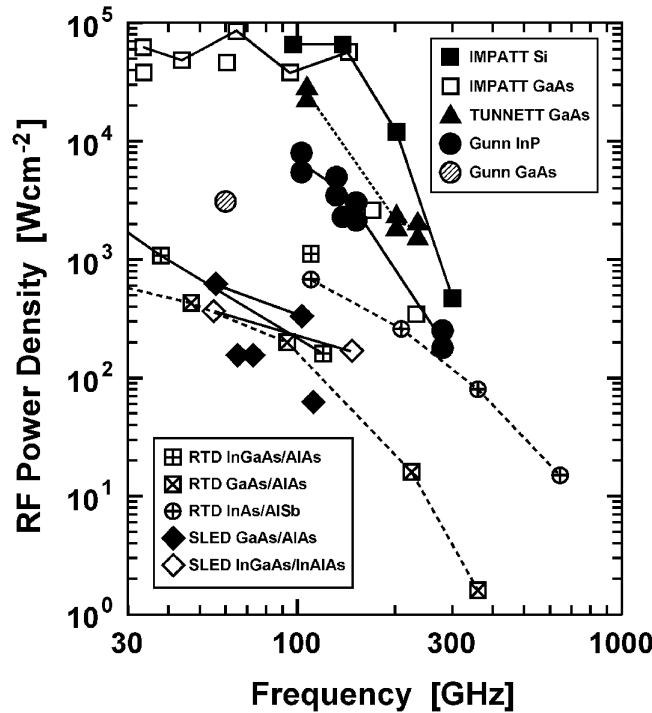


Fig. 3. RF power densities Φ_{RF} in two-terminal devices as derived from published state-of-the-art results. Due to uncertainties in device areas, ranges are given for Φ_{RF} of InP Gunn devices and GaAs TUNNETT diodes at particular frequencies. Lines between data points at different frequencies are only as a guide to the eye.

3. TRANSIT-TIME DIODES

Si IMPATT diodes were the first semiconductor devices to generate RF power above 300 GHz. As shown in Fig. 4 (and in conjunction with Fig. 1 and Fig. 5), they yielded the highest RF power levels from any solid-state fundamental RF source up to 300 GHz. Exemplary RF power levels (and corresponding dc-to-RF conversion efficiencies) of 50 mW (1.3%) at 202 GHz [20]; 44 mW (1.2%) at 214 GHz [20]; 50 mW (<2%) at 217 GHz [21]; [22], 50 mW (<1%) at 245 GHz [22]; 12 mW (<0.5%) at 255 GHz [22]; 7.5 mW (0.35%) at 285 GHz [23]; 1.2 mW (<0.05%) at 301 GHz [20]; and 0.2 mW at 361 GHz [23] were measured at very high operating junction temperatures of typically more than 300 °C with waveguide circuits at room temperature [21]. Higher RF power levels of, *e.g.*, 4.5 mW (0.13%) at 295 GHz and 2.2 mW (0.047%) at 412 GHz, but also higher oscillation frequencies of up to 430 GHz were attained by cooling the heat sink of the diode and the waveguide circuit to 77 K (liquid nitrogen) [24].

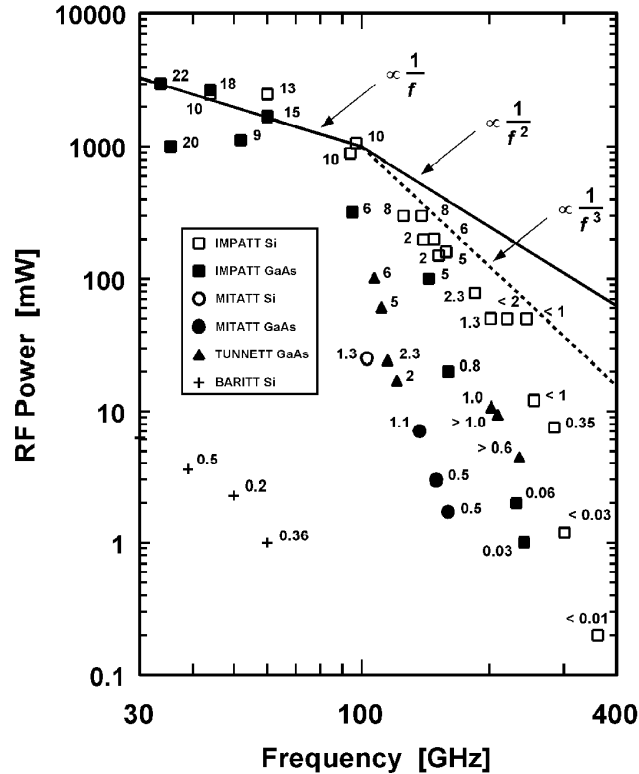


Fig. 4. Published state-of-the-art results from Si and GaAs transit-time diodes under CW operation in the frequency range of 30–400 GHz. Numbers next to the symbols denote dc-to-RF conversion efficiencies in percent.

Impact ionization as the carrier generation mechanism in IMPATT diodes is a major contributor to the noise of free-running oscillators compared to, *e.g.*, the smaller contri-

tribution from mainly thermal noise in the domain formation process of Gunn devices [1], [2]. Therefore, IMPATT diodes are generally considered quite noisy, although techniques are known on how to reduce noise contributions from impact ionization at the price of typically lower dc-to-RF conversion efficiencies [1], [2]. The noise properties of IMPATT diodes restrict their use as local oscillator (LO) sources to either receiver applications where the highest sensitivity is not of primary concern or sensitive low-noise receivers in which well-balanced Schottky diodes as subharmonically pumped mixers cancel out the noise from the LO [25].

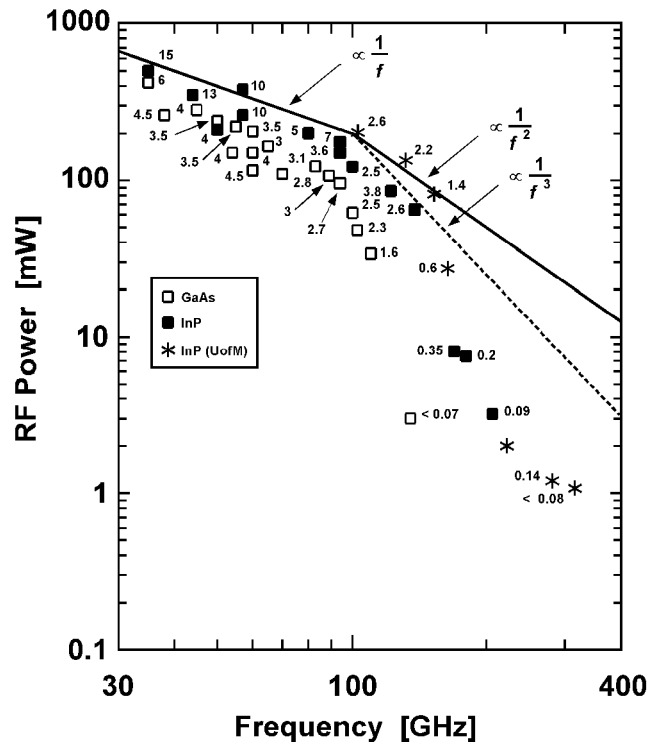


Fig. 5. Published state-of-the-art results from GaAs and InP Gunn devices under CW operation in the frequency range of 30–400 GHz. Numbers next to the symbols denote dc-to-RF conversion efficiencies in percent.

TUNNETT diodes, on the other hand, are based on a fast and quiet primary carrier injection mechanism [1], [2], which makes them another prime candidate for RF generation at high millimeter-wave and submillimeter-wave frequencies. RF power levels of 100 ± 5 mW (and corresponding dc-to-RF conversion efficiencies of around 6%) were measured with GaAs TUNNETT diodes on diamond heat sinks in the fundamental mode at oscillation frequencies of 100–107 GHz [19].

Power extraction at higher harmonic frequencies was investigated with Si [20], [26] and GaAs [27], [28] IMPATT diodes as well as GaAs TUNNETT diodes [19] [29]. Diode

structures and properties suggest operation in second- or even third-harmonic mode for some of the aforementioned state-of-the-art results from Si IMPATT diodes above 200 GHz. As an example, the RF power of 1.2 mW at 301 GHz was thought to be generated at the third-harmonic frequency [20], but for many other results at these high millimeter-wave frequencies, no attempts to determine the exact mode of operation were reported.

The aforementioned GaAs TUNNETT diodes were also operated in a second-harmonic mode up to 237 GHz and yielded RF power levels exceeding 10 mW at 202 GHz, 9 mW around 210 GHz, and 4 mW around 235 GHz [29], [30]. These power levels correspond to dc-to-RF conversion efficiencies around 1% at 202 GHz and 210 GHz as well as above 0.6% around 235 GHz [29], [30]. The diodes operate as self-oscillating multipliers with a large modulation of the depletion region, which is akin to that of high-performance varactor diodes and is responsible for the high up-conversion efficiencies of more than 20% [29]. This mode of operation also reaches its performance peak below the maximum permissible bias current density [29]. Therefore, higher RF power levels and higher operating frequencies are expected from TUNNETT diodes that are designed for this mode of operation and have shorter active regions as well as doping concentrations appropriate for higher current densities. Simulations also indicated that RF power levels of the order of 10 mW can be generated in the 240–280 GHz frequency range with GaAs single-drift TUNNETT diodes in the fundamental mode [31].

The measured RF power levels and, particularly, conversion efficiencies of these TUNNETT diodes in a second-harmonic mode are comparable to those obtained from frequency multipliers where, *e.g.*, Schottky-barrier varactor diodes are driven by Gunn devices [32], [33]. Fig. 6 compares these results from various frequency multipliers in the 100–1000 GHz frequency range with select results from GaAs TUNNETT diodes, InP Gunn devices, and RTDs. In addition, very clean spectra were recorded from these GaAs TUNNETT diodes in the fundamental as well as in a second-harmonic mode [19], [29], [30]. TUNNETT diodes also yielded the lowest small-signal frequency-modulation (FM) noise measure reported from any oscillator with a two-terminal device [1], [19].

Contrary to preliminary results from GaAs TUNNETT diodes [19], a very preliminary study of the properties of single-drift GaAs IMPATT diodes in a second-harmonic mode found that the measured spectra of free-running oscillators with these diodes [28] were clearly not as clean as those of free-running oscillators with TUNNETT diodes (or Gunn devices). This result was indeed expected from approximately 7–8 dB higher values of the small-signal FM noise measure and at least 6 dB higher values of the large-signal FM noise measure of GaAs single-drift IMPATT diodes in the fundamental mode at *W*-band frequencies [1], [19]. Furthermore, dc-to-RF conversion efficiencies of, *e.g.*, 0.04% at 194 GHz [28] or 0.06% at 232 GHz [27] were inferior to those of the TUNNETT diodes in a similar circuit configuration [19], [29].

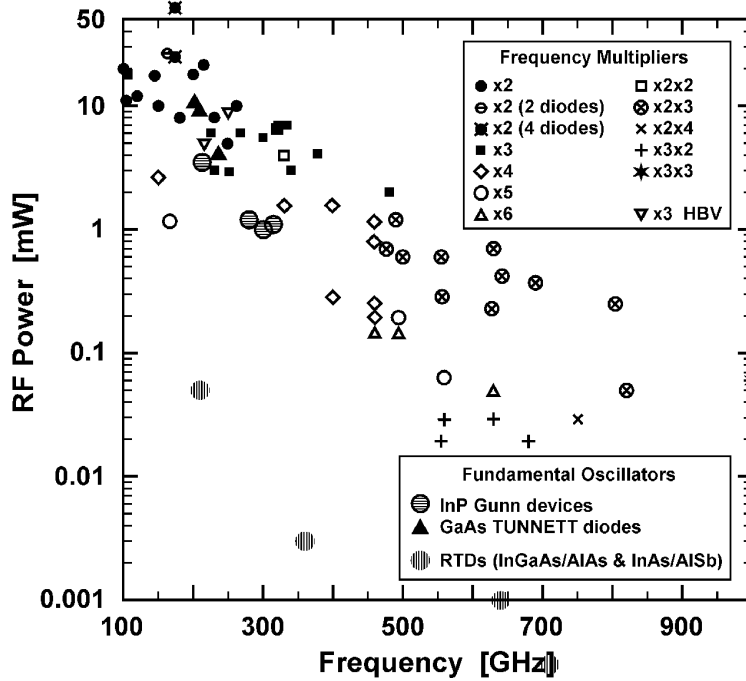


Fig. 6. Published state-of-the-art results from frequency multipliers with GaAs Schottky-barrier or InP-based heterojunction-barrier varactor diodes in the 100–1000 GHz frequency range in comparison with published state-of-the-art results from GaAs TUNNETT diodes, InP Gunn devices, and RTDs above 200 GHz.

4. TRANSFERRED-ELECTRON DEVICES

GaAs or InP transferred-electron (or Gunn) devices are quite frequently employed in all-solid-state LO sources for submillimeter-wave frequencies, where they generate RF power at medium millimeter-wave frequencies of 60–150 GHz and then drive one or more stages of frequency multipliers with Schottky-barrier varactor diodes [25], [32], [33] or, more recently, heterojunction-barrier varactor diodes [34]. More than ten semiconductor materials in the III-V and II-VI groups are known to exhibit the transferred-electron effect, [2], [35], however, so far, only GaAs and InP have been exploited commercially. GaAs Gunn devices are not a topic of this paper since only InP Gunn devices yield RF power above 200 GHz.

The highest dc-to-RF conversion efficiencies at low to medium millimeter-wave frequencies and excellent performance up to *D*-band frequencies were reported from InP TEDs with $n\bar{n}^+$ layer structures and current-limiting contacts at the cathode side of the active region. Examples of RF power levels (and corresponding conversion efficiencies) are 380 mW at 57 GHz (10.6%) in the fundamental mode [36] as well as 175 mW (7%) at 94 GHz, 85 mW (3.8%) at 125 GHz, and 65 mW (2.6%) at 138 GHz in a second-

harmonic mode [37], [38]. As shown in Fig. 5, the highest RF power levels from any Gunn device above 100 GHz were achieved with devices that had an $n^+n^-n^+$ layer structure as well as a graded doping profile in the active region and were mounted on diamond heat sinks [19], [35], [39]. Operation in the fundamental mode was observed up to 165 GHz. As examples, RF power levels (and corresponding dc-to-RF conversion efficiencies) exceeded 200 mW (2.6%) at 103 GHz [35]; 130 mW (2.2%) at 132 GHz; 80 mW (1.4%) at 152 GHz; and 30 mW at 162 GHz [19], [35]. High RF power levels and excellent noise performance [1], [19], [30], [35], [39] make these InP Gunn devices ideally suited for driving high-performance Schottky-diode frequency multipliers in sensitive terahertz receivers.

Operation in a second-harmonic mode helps overcome the inherent fundamental frequency limit in Gunn devices. RF power levels of more than 3.5 mW at 214 GHz, more than 2 mW around 220 GHz, as well as more than 1 mW up to 315 GHz were measured in this mode of operation [30], [40]. The RF power levels above 300 GHz are the highest reported to date from any solid-state fundamental RF source and, as can be seen from Fig. 6, they approach those from frequency multipliers [32]. These RF power levels even exceed early performance predictions [41]–[44], but the results of more recent simulations indicate that significant increases in RF power levels can be expected from more optimized device structures and circuits up to at least 320 GHz [45], [46]. Fig. 7 compares the experimental results in the fundamental mode, as well as those in a second-harmonic mode with these recent predictions from detailed simulations [46] that employed a Monte Carlo-based harmonic balance technique [45]. Monte-Carlo simulations were originally used in the design of the *D*-band structures [47] and showed good agreement between performance predictions and measured results [45], [48]. Various device structures, which were designed for operation in a second-harmonic mode in the 200–310 GHz frequency range and had a doping gradient in the active region as shown schematically in the inset of Fig. 7, were investigated [46], [49].

The measured RF power levels in the fundamental mode at *D*-band frequencies and the predicted RF power levels for operation in a second-harmonic mode at *J*-band (220–325 GHz) frequencies follow a clear $1/f^3$ roll-off up to about 300 GHz. This trend evidently shows that substantial performance improvements can be expected from optimized device structures and waveguide circuits at *J*-band frequencies. The trend above 300 GHz may also indicate that the transferred-electron effect in InP could be utilized even above 320 GHz and possibly up to 500 GHz [49] with devices operating in a second- or third-harmonic mode. In addition, the experimental results from InP Gunn devices above 220 GHz imply that the derivations of fundamental physical frequency limits for the transferred-electron effect in InP should be revisited and re-investigated in greater detail.

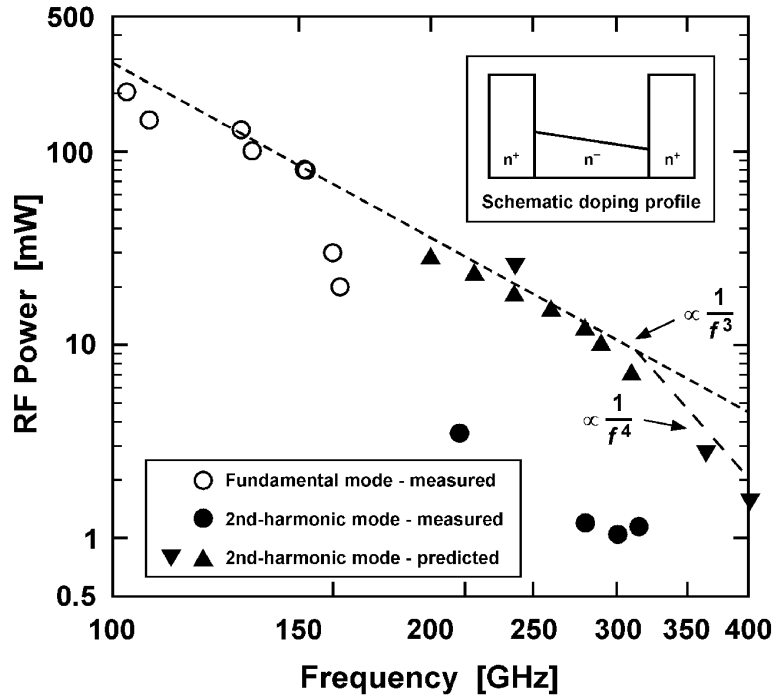


Fig. 7. Comparison of predicted [45], [46], [49] and measured [19], [40] CW RF power levels from InP Gunn devices with an $n^+n^-n^+$ structure and a doping gradient in the active region as shown in the inset for the 100–320 GHz frequency range.

5. CONCLUSIONS

RF power generating capabilities of several two-terminal devices were reviewed and compared. Compared to GaAs, InP is the better semiconductor material system to reach submillimeter-wave frequencies with Gunn devices. Experimental results from both GaAs and InP Gunn devices indicate that the fundamental frequency limit of the transferred-electron effect may be higher than previously thought. More detailed studies are necessary to determine the ultimate fundamental frequency limit, *i.e.*, if InP Gunn devices are capable of generating significant RF power levels in the 320–400 GHz frequency range. Nonetheless, simulations predict that substantial performance improvements are feasible at *J*-band frequencies, which may help eliminate one or two stages in a multiplier chain to reach terahertz frequencies.

As can be seen from the published results in Figs. 1, 4, and 6, the RF power levels from InP Gunn devices on diamond heat sinks are the highest reported to date from any solid-state fundamental RF source operated at room temperature and for frequencies above 300 GHz. Likewise, GaAs TUNNETT diodes are considered the second-most powerful solid-state fundamental RF source operated at room temperature and for frequencies above 200 GHz.

Reliable long-term operation requires the heat dissipation in the device to be minimized. Both Gunn devices and TUNNETT diodes on diamond heat sinks meet these requirements since the above-mentioned state-of-the-art-results were obtained at “cool” operating active-layer temperatures estimated to be generally below 200 °C, but most often well below 150 °C [1], [29], [30],[35], [39], [40], [48].

Other semiconductor material systems, such as GaN or InN, are known to exhibit a transferred-electron effect [35] which could be utilized for millimeter-wave Gunn devices. However, various Monte Carlo simulations predict its onset to occur in these semiconductor materials at five to more than ten times higher threshold electric fields than in InP [50]–[53]. Furthermore, much smaller values for the negative differential mobility at electric fields above twice the threshold field, as well as lower values for the low-field electron mobility, require much higher doping \times length products for rapid domain formation than in GaAs or InP. Higher electric fields and, as a result, bias voltages, will enhance the RF power generating capabilities, but, together with higher doping \times length products, may cause dc input power densities that are at least one order of magnitude higher than in InP and, even on diamond heat sinks, result in extreme overheating in the device. As a consequence, major advances in material growth, material characterization, and experimental verification of material properties and parameters, as well as appropriate device fabrication technologies, are required before the potential and capabilities of any of these material systems can be assessed fully and eventually utilized.

ACKNOWLEDGMENTS

Funding from JPL under contracts 961299 and 961527 as well as from NSF under grant ECS 98-03781 is kindly acknowledged.

REFERENCES

- [1] H. Eisele and G. I. Haddad, “Active Microwave Diodes,” in *Modern Semiconductor Devices*, S. M. Sze, Ed., Ch. 6, John Wiley & Sons, New York, 1997, pp. 343–407.
- [2] S. M. Sze, *Physics of Semiconductor Devices*, 2nd Ed., John Wiley & Sons, New York, 1981.
- [3] L. Esaki and R. Tsu, “Superlattice and negative differential conductivity in semiconductors,” *IBM J. Res. Develop.*, **14**(1), 1970, pp. 61–65.
- [4] L. L. Chang, L. Esaki, and R. Tsu, “Resonant tunneling in semiconductor double-barriers,” *Appl. Phys. Lett.*, **24**(12), 1974, pp. 593–595.
- [5] B. Agarwal, A. E. Schmitz, J. J. Brown, M. Matloubian, M. G. Case, M. Le, M. Lui, and M. J. W. Rodwell, “112-GHz, 157-GHz, and 180-GHz InP HEMT traveling-wave amplifiers,” *IEEE Trans. Microwave Theory Tech.*, **46**(12), 1998, pp. 2553–2559.

- [6] S. Weinreb, T. Gaier, R. Lai, M. Barsky, Y. C. Leong, and L. Samoska, "High-gain 150–215-GHz MMIC amplifier with integral waveguide transitions," *IEEE Microwave Guided Wave Lett.*, **9**(7), 1999, pp. 282–284.
- [7] R. Lai, M. Barsky, T. Huang, M. Sholley, H. Wang, Y. L. Kok, D. C. Streit, T. Block, P. H. Liu, T. Gaier, and L. Samoska, "An InP HEMT MMIC LNA with 7.2-dB gain at 190 GHz," *IEEE Microwave Guided Wave Lett.*, **8**(11), 1998, pp. 393–395.
- [8] Q. Lee, B. Agarwal, D. Mensa, R. Pallela, J. Guthrie, L. Samoska, and M. J. W. Rodwell, "A > 400 GHz f_{\max} transferred-substrate heterojunction bipolar transistor IC technology," *IEEE Electron Device Lett.*, **19**(3), 1998, pp. 77–79.
- [9] D. Mensa, Q. Lee, J. Guthrie, S. Jaganathan, and M. J. W. Rodwell, "Transferred-substrate HBTs with 254 GHz f_t ," *Electron. Lett.*, **35**(7), 1999, pp. 288–290.
- [10] Y. C. Chen, D. L. Ingram, R. Lai, M. Barsky, R. Grunbacher, T. Block, H. C. Yen, and D. C. Streit, "A 95-GHz InP HEMT MMIC amplifier with 427-mW power output," *IEEE Microwave Guided Wave Lett.*, **8**(11), 1998, pp. 399–401.
- [11] Y. Kwon, D. Pavlidis, T. L. Brock, and D.C. Streit, "A D-band monolithic fundamental oscillator using InP-based HEMT's," *IEEE Trans. Microwave Theory Tech.*, **41**(12), 1993, pp. 2336–2344.
- [12] S. E. Rosenbaum, B. K. Kormanyos, L. M. Jelloian, M. Matloubian, A. S. Brown, L. E. Larson, L. D. Nguyen, M. A. Thompson, L. P. B. Katehi, and G. M. Rebeiz, "155- and 213-GHz All-nAs/GaInAs/InP HEMT MMIC oscillators," *IEEE Trans. Microwave Theory Tech.*, **43**(4), 1995, pp. 927–933.
- [13] E. R. Brown, C. D. Parker, A. R. Calawa, M. J. Manfra, C. L. Chen, L. J. Mahoney, and W. D. Goodhue, "High-frequency resonant-tunneling oscillators," *Microwave Optical Technol. Lett.*, **4**(1), 1991, pp. 19–23.
- [14] E. R. Brown, J. R. Söderström, C. D. Parker, L. J. Mahoney, K. M. Molvar, and T. C. McGill, "Oscillations up to 712 GHz in InAs/AlSb resonant tunneling diodes," *Appl. Phys. Lett.*, **58**(20), 1991, pp. 2291–2293.
- [15] E. Schomburg, J. Grenzer, K. Hofbeck, T. Blomeier, S. Winnerl, S. Brandl, A. A. Ignatov, K. F. Renk, D. G. Pavel'ev, Yu. Koschurinov, V. Ustinov, A. Zhukov, A. Kovsch, S. Ivanov, and P. S. Kop'ev, "Millimeter wave generation with a quasi planar superlattice electronic device," *Solid-State Electron.*, **42**(7–8), 1998, pp. 1495–1498.
- [16] S. Brandl, E. Schomburg, R. Scheuerer, K. Hofbeck, J. Grenzer, K. F. Renk, D. G. Pavel'ev, Yu. Koschurinov, A. Zhukov, A. Kovsch, V. Ustinov, S. Ivanov, and P. S. Kop'ev, "Millimeter wave generation by a self-sustained current oscillation in an InGaAs/InAlAs superlattice," *Appl. Phys. Lett.*, **73**(21), 1998, pp. 3177–3119.
- [17] E. Schomburg, M. Henini, J. M. Chamberlain, D. P. Steenson, S. Brandl, K. Hofbeck, K. F. Renk, and W. Wegscheider, "Self-sustained current oscillation above 100 GHz in a GaAs/AlAs superlattice," *Appl. Phys. Lett.*, **74**(15), 1999, pp. 2179–2181.
- [18] E. Schomburg, R. Scheuerer, S. Brandl, K. F. Renk, D. G. Pavel'ev, Yu. Koschurinov, V. Ustinov, A. Zhukov, A. Kovsch, and P. S. Kop'ev, "InGaAs/InAlAs superlattice oscillator at 147 GHz," *Electron. Lett.*, **35**(17), 1999, pp. 1491–1492.
- [19] H. Eisele and G. I. Haddad, "Two-terminal millimeter-wave sources," *IEEE Trans. Microwave Theory Tech.*, **46**(6), 1998, pp. 739–746.
- [20] T. Ishibashi and M. Ohmori, "200-GHz 50-mW CW oscillation with silicon SDR IMPATT diodes," *IEEE Trans. Microwave Theory Tech.*, **24**(11), 1976, pp. 858–859.

- [21] N. B. Kramer and R.A. Johnson, "Generating power at mm-wave frequencies," *Microwaves & RF*, **23**(5), 1984, pp. 243–249.
- [22] K. Chang, W. F. Thrower, and G. M. Hayashibara, "Millimeter-wave silicon IMPATT sources and combiners for the 110-260-GHz range," *IEEE Trans. Microwave Theory Tech.*, **29**(12), 1981, pp. 1278–1284.
- [23] M. Ino, T. Ishibashi, and M. Ohmori, "C.W. oscillation with p⁺-p-n⁺ silicon IMPATT diodes in 200 GHz and 300 GHz bands," *Electron. Lett.*, **12**(6), 1976, pp. 148–149.
- [24] T. Ishibashi, M. Ino, T. Makimura, and M. Ohmori, "Liquid-nitrogen-cooled submillimeter-wave silicon IMPATT diodes," *Electron. Lett.*, **13**(10), 1977, pp. 299–300.
- [25] I. Mehdi, P. H. Siegel, D. A. Humphrey, T. H. Lee, R. J. Dengler, J. E. Oswald, A. Pease, R. Lin, H. Eisele, R. Zimmermann, and N. Erickson, "An all solid-state 640 GHz subharmonic mixer," *IEEE MTT-S Int. Microwave Symp. Dig.*, Baltimore, MD, June 7–12, 1998, pp. 403–406.
- [26] M. Ohmori, T. Ishibashi, and S. Ono, "Dependency of the highest harmonic oscillation frequency on junction diameter of IMPATT diodes," *IEEE Trans. Electron Devices*, **24**(12), 1977, pp. 1323–1329.
- [27] H. Böhm, J. Freyer, and M. Claassen, "CW harmonic power generation of GaAs IMPATT diodes above 200 GHz," *Proc. Terahertz Spectroscopy Applications II*, Munich, Germany, SPIE **3828**, 1999, pp. 81–88.
- [28] H. Eisele, unpublished results.
- [29] H. Eisele, "Efficient second-harmonic power extraction from GaAs TUNNETT diodes above 200 GHz," *Electron. Lett.*, **34**(13), 1998, pp. 1324–1326 **and** *Electron. Lett.*, **34**(15), 1998, pp. 1531.
- [30] H. Eisele, A. Rydberg, and G. I. Haddad: "Recent Advances in the Performance of InP Gunn Devices and GaAs TUNNETT Diodes for the 100–300-GHz Frequency Range and Above," *Special Issue on Terahertz Electronics, IEEE Transactions on Microwave Theory and Techniques*, vol. 48, no. 4, pp. 626–631, April 2000.
- [31] C-C. Chen, R. K. Mains, G. I. Haddad, and H. Eisele, "Numerical simulation of TUNNETT and MITATT devices in the millimeter and submillimeter range," *Proc. 4th Int. Symp. Space Terahertz Technol.*, Los Angeles, CA, March 30–April 1, 1993, pp. 362–376.
- [32] A. V. Räisänen, "Frequency multipliers for millimeter and submillimeter wavelengths," *Proc. IEEE*, **80**(11), 1992, pp. 1842–1852.
- [33] T. W. Crowe, T. C. Grein, R. Zimmermann, and P. Zimmermann, "Progress toward solid-state local oscillators at 1 THz," *IEEE Microwave Guided Wave Lett.*, **6**(5), 1996, pp. 207–208.
- [34] X. Mélique, A. Maestrini, P. Mounaix, M. Favreau, O. Vanbésien, J.M. Goutoule, G. Beaudin, T. Nähri and D. Lippens, "Record performance of a 250 GHz InP-based heterostructure barrier varactor tripler," *Electron. Lett.*, **35**(11), 1999, pp. 938–939.
- [35] H. Eisele, "Gunn or transferred-electron devices," in *Encyclopedia of Electrical and Electronics Engineering*, J. G. Webster, Ed., vol. 8, John Wiley & Sons, New York, 1999, pp. 523–537.
- [36] B. Fank, J. Crowley, and C. Hang, "InP Gunn diode sources," *Millimeter Wave Technology III*, SPIE **544**, 1985, pp. 22–28.
- [37] J. D. Crowley, C. Hang, R. E. Dalrymple, D. R. Tringali, F. B. Fank, and L. Wandinger, "140 GHz indium phosphide Gunn diode," *Electron. Lett.*, **30**(6), 1994, pp. 499–500.

- [38] J. D. Crowley, R. E. Dalrymple, C. Hang, D. R. Tringali, F. B. Fank, and L. Wandinger, "InP Gunn diodes serve millimeter-wave applications," *Microwaves & RF*, **33**(3), 1994, pp. 143–146.
- [39] H. Eisele and G. I. Haddad, "High-performance InP Gunn devices for fundamental-mode operation in D-band (110–170 GHz)," *IEEE Microwave Guided Wave Lett.*, **5**(11), 1995, pp. 385–387.
- [40] H. Eisele, "Second-harmonic power extraction from InP Gunn devices with more than 1 mW in the 260–320 GHz frequency range," *Electron. Lett.*, **34**(25), 1998, pp. 2412–2413.
- [41] L. Wandinger, "mm-wave InP Gunn devices: status and trends," *Microwave J.*, **24**(3), 1981, pp. 71–78.
- [42] I. G. Eddison, "Indium phosphide and gallium arsenide transferred-electron devices," in *Infrared and Millimeter Waves*, Vol. 11, *Millimeter Components and Techniques, Part III*, Academic Press, Orlando, 1984, pp. 1–59.
- [43] P. A. Rolland, G. Salmer, E. Constant, and R. Fauquembergue, "Comparative frequency behavior of GaAs, InP, and GaInAs transferred-electron devices—derivation of a simple comparative criterion," *IEEE Trans. Electron Devices*, **28**(3), 1981, pp. 341–343.
- [44] M. R. Friscourt and P.A. Rolland, "Optimum design of n^+n-n^+ InP devices in the millimeter-range frequency limitation—RF performances," *IEEE Electron Device Lett.*, **4**(5), 1983, pp. 135–137.
- [45] R. Kamoua, "Monte Carlo-based harmonic balance technique for the simulation of high-frequency TED oscillators," *IEEE Trans. Microwave Theory Tech.*, **46**(10), 1998, pp. 1376–1381.
- [46] R. Kamoua, "Potential of second-harmonic power generation in InP Gunn oscillators above 200 GHz," *Proc. 4th Int. Conf. Millimeter Submillimeter Waves Applications*, San Diego, California, July 20–24, 1998, pp. 32–37.
- [47] R. Kamoua, H. Eisele, and G. I. Haddad, "D-band (110–170 GHz) InP Gunn devices," *Solid-State Electron.*, **36**, 1993, pp. 1547–1555.
- [48] H. Eisele and G. I. Haddad, "Recent advances in the performance of GaAs- and InP-based two-terminal devices as high-power millimeter-wave sources," *Proc. 4th Int. Conf. Millimeter Wave Far Infrared Science Technol.*, Beijing, China, August 12–15, 1996, pp. 2–5.
- [49] R. Kamoua and H. Eisele, "Power generation with fundamental and second-harmonic mode InP Gunn oscillators—performance above 200 GHz and upper frequency limits," these proceedings.
- [50] J. Kolnik, I. H. Oğuzman, K. F. Brennan, R. Wang, P. P. Ruden, and Y. Wang, "Electronic transport studies of bulk zincblende and wurtzite phases of GaN based on an ensemble Monte Carlo calculation including a full zone band structure," *J. Appl. Phys.*, **78**(2), 1995, pp. 1033–1038.
- [51] U. V. Bhapkar and M. S. Shur, "Monte Carlo calculation of velocity-field characteristics of wurtzite GaN," *J. Appl. Phys.*, **82**(4), 1997, pp. 1649–1655.
- [52] S. Krishnamurthy, M. van Schilfgaarde, A. Sher, and A.-B. Chen, "Bandstructure effect on high-field transport in GaN and GaAlN," *Appl. Phys. Lett.*, **71**(14), 1997, pp. 1999–2001.
- [53] E. Bellotti, B. K. Doshi, K. F. Brennan, J. D. Albrecht, and P. P. Ruden, "Ensemble Monte Carlo study of electron transport in wurtzite InN," *J. Appl. Phys.*, **85**(2), 1999, pp. 916–923.